Development of Heart Failure and Congenital Septal Defects in Mice Lacking Endothelial Nitric Oxide Synthase

Qingping Feng, MD, PhD; Wei Song, MD, PhD; Xiangru Lu, MD; Joel A. Hamilton, BSc; Ming Lei, MD; Tianqing Peng, MD; Siu-Pok Yee, PhD

Background—Nitric oxide (NO) produced by endothelial NO synthase (eNOS) plays an important role in the regulation of cell growth, apoptosis, and tissue perfusion. Recent studies showed that mice deficient in eNOS developed abnormal aortic bicuspid valves. The aim of the present study was to additionally investigate the role of eNOS in heart development.

Methods and Results—We examined postnatal mortality, cardiac function, and septum defects in $eNOS^{-/-}$, $eNOS^{+/-}$, and wild-type mice. Postnatal mortality was significantly increased in $eNOS^{-/-}$ (85.1%) and $eNOS^{+/-}$ (38.3%) compared with wild-type mice (13.3%, $P<0.001$). Postmortem examination found severe pulmonary congestion with focal alveolar edema in mice deficient in eNOS. Heart shortening determined by ultrasound crystals was significantly decreased in $eNOS^{-/-}$ compared with wild-type mice ($P<0.05$). Congenital atrial and ventricular septal defects were found in neonatal hearts. The incidence of atrial or ventricular septal defects was significantly increased in $eNOS^{-/-}$ (75%) and $eNOS^{+/-}$ (32.4%) neonates compared with those of the wild-type mice (4.9%). At embryonic days 12.5 and 15.5, cardiomyocyte apoptosis and myocardial caspase-3 activity were increased in the myocardium of $eNOS^{-/-}$ compared with wild-type embryos ($P<0.01$), and increases in apoptosis persisted to neonatal stage in $eNOS^{-/-}$ mice.

Conclusions—Deficiency in eNOS results in heart failure and congenital septal defects during cardiac development, which is associated with increases in cardiomyocyte apoptosis. Our data demonstrate that eNOS plays an important role in normal heart development. **(*Circulation*. 2002;106:873-879.)**

Key Words: nitric oxide ■ heart failure ■ heart defects, congenital ■ heart septal defects ■ apoptosis

Nitric oxide (NO) is produced from the guanidino group of L-arginine in an NADPH-dependent reaction catalyzed by a family of NO synthase (NOS) enzymes.[1] There are at least 3 distinct isoforms of NOS: neural NOS (nNOS), inducible NOS (iNOS), and endothelial NOS (eNOS).[2] The neuronal isoform is highly expressed in neuronal cells and skeletal muscle, whereas the inducible isoform is expressed in many cell types primarily in response to inflammatory cytokines. The endothelial isoform originally was identified in endothelial cells. NO produced by eNOS plays an important role in the regulation of cell growth and apoptosis as well as vasodilation and antithrombotic actions.[2] Cardiomyocytes constitutively express eNOS starting from early embryonic stages and produce NO under normal physiological conditions.[3–5] NO produced from cardiomyocytes may enhance myocardial relaxation and regulate contractility as well as coronary perfusion.[6,7] It has also been shown that eNOS is involved in cardiomyogenesis and formation of limb vasculature during embryogenesis.[3,8]

NO produced from eNOS protects cell from apoptosis. Exposure to low concentrations of NO donors or stimulation of endogenous NO release has been demonstrated to decrease apoptosis in hepatocytes and endothelial cells by inhibiting caspase-3 activation.[9,10] Apoptosis is a highly regulated physiological process in normal heart development. During early embryonic and postnatal heart development, apoptosis is demonstrated in various areas of the heart.[11–15] Increases in myocardial apoptosis during embryonic development result in cardiac dysfunction and congenital heart defects.[11] In the present study, we wished to examine the hypothesis that deficiency in eNOS results in myocardial apoptosis, which leads to cardiac dysfunction.

Development of the atrioventricular septal area is highly complex. Multiple primordia contribute to a central mesenchymal mass, including the mesenchyme on the leading edge of the primary atrial septum, the atrioventricular endocardial cushions, and the cap of mesenchyme on the spina vestibuli. Fusion of these components closes the ostium primum, completing atrial and atrioventricular septation.[16] The molecular mechanisms that govern the formation of atrioventricular septal area remain largely unknown. Recent studies showed

Received January 8, 2002; revision received May 15, 2002; accepted May 15, 2002.

From the Departments of Medicine, Physiology, Pharmacology, and Toxicology, Cardiology Research Laboratory, London Health Sciences Centre; and Departments of Oncology and Biochemistry, Cancer Research Laboratories, London Regional Cancer Center (S.-P.Y.), University of Western Ontario, London, Ontario, Canada.

Correspondence to Dr Qingping Feng, Department of Medicine, London Health Sciences Centre, Victoria Campus, 375 South St, London, Ontario, Canada N6A 4G5. E-mail qfeng@uwo.ca

Circulation **is available at http://www.circulationaha.org** **DOI: 10.1161/01.CIR.0000024114.82981.EA**

that mice deficient in eNOS developed aortic bicuspid valves.[17] In the present study, we additionally demonstrated that deficiency in NO results in congenital atrial and ventricular septal defects in mice. Our results suggest that NO plays an important role during cardiac development.

Methods

Animals

Breeding pairs of *eNOS*$^{-/-}$ (stock No. 002684) and wild-type C57BL/6 (*eNOS*$^{+/+}$) mice were purchased from Jackson Laboratory (Bar Harbor, Maine). A breeding program was carried out to produce neonates. To generate *eNOS*$^{+/-}$ mice, *eNOS*$^{-/-}$ animals were bred with *eNOS*$^{+/+}$ mice. Genotyping of *eNOS*$^{+/-}$ and *eNOS*$^{-/-}$ mice was performed by a polymerase chain reaction (PCR) method using genomic DNA prepared from tail biopsies. All procedures involving mouse husbandry and manipulation were in accordance with the guidelines of the Canadian Council of Animal Care and approved by the Animal Use Subcommittee at the University of Western Ontario, Canada.

Histology, Microdissections, and Scanning Electron Microscopy

Neonatal *eNOS*$^{-/-}$, *eNOS*$^{+/-}$, and *eNOS*$^{+/+}$ mice were used for analysis. Neonatal hearts and lungs were isolated and fixed in 10% buffered formalin, dehydrated, and embedded in paraffin. Serial heart sections were made, stained with hematoxylin and eosin, and examined by light microscopy. To quantify the incidence of septal defects, neonatal hearts (36 *eNOS*$^{-/-}$, 34 *eNOS*$^{+/-}$, and 41 *eNOS*$^{+/+}$) were fixed in 10% buffered formalin, and a standard procedure for microdissection of the heart was applied according to methods described previously.[18,19] Briefly, the heart was exposed and examined under an operating microscope. The right ventricle was dissected with crafted microscissors proceeding from the apex to the pulmonary artery trunk. Similarly, the left ventricle was opened from the apex toward the base of heart and its internal relief examined. Subsequently, the parietal segments of ventricles and atria were isolated by extending the previously mentioned cuts of the right and left ventricles beyond the base of the heart. The ventricular cavity and the septum were scrutinized for anomalies. Hearts were dehydrated by graded methanol solutions, dried by a critical point dryer (Polaron E3000, Watford Hertfordshire), sputtered with gold coating, and examined by a field emission scanning electron microscope (S-4500, Hitachi).

Measurement of Neonatal Cardiac Shortening In Vivo

Postnatal day 1 (P1) mice were anesthetized with sodium pentobarbital (75 mg/kg, IP). After tracheotomy, the trachea was cannulated with a PE10 catheter, which was connected to a ventilator (SAR-830, CWE Inc). Mice were artificially ventilated with room air. Tidal volume was set at 25 μL with 90 breaths/min and 40/60 inspiration/expiration ratio. Body temperature was maintained at 37°C. The heart was exposed through a midline sternotomy. The crystals (0.7 mm) were fixed on the heart surface to allow short-axis measurement similarly, as we previously described in adult mice.[20] The ultrasound signals were measured by a Digital Sonomicrometer (Sonometrics). Maximum and minimum distances as well as percent shortening were calculated.

In Situ Detection of Apoptotic Cells

To localize and quantitatively assess cells undergoing apoptosis in the heart, a terminal deoxynucleotidyl transferase (TdT)-mediated dUTP nick-end labeling (TUNEL) assay was performed on paraffin-embedded sections from embryonic day (E) 12.5 mice using an in situ apoptosis detection kit (Roche Molecular Biochemicals) according to our previous report.[21]

Enzyme Immunoassay for Cytoplasmic Histone-Associated DNA Fragments

For quantitative determination of apoptosis, we measured cytoplasmic histone-associated DNA fragments (mononucleotides and oligonucleotides) in E12.5, E15.5, and P1 mouse hearts using a photometric enzyme immunoassay (Cell Death Detection ELISA, Roche Molecular Biochemicals), as we described previously.[21]

Caspase-3 Activity

Fetal myocardial caspase-3 activity was measured using a caspase-3 fluorescent assay kit according to manufacturer's protocol (BIOMOL Research Laboratories). Briefly, 5 to 7 hearts isolated from E12.5 or E15.5 mice were pooled together and homogenized, and protein concentration was determined by Bradford method.[22] Samples (50 μg protein) in duplicates were incubated with caspase-3 substrate Ac-DEVD-AMC or Ac-DEVD-AMC plus inhibitor AC-DEVD-CHO at 37°C for 2 hours before measurements were made by a fluorescent spectrophotometer (excitation at 380 nm, emission at 405 nm). Signals from inhibitor-treated samples served as background.

Statistical Analysis

Data are presented as mean±SEM. Student's *t* test, χ^2 analysis, and ANOVA followed by Student-Newman-Keuls test were performed. Survival curves were created by the method of Kaplan and Meier and compared by log-rank test. $P<0.05$ was considered statistically significant.

Results

Postnatal Survival and Cardiac Function

Postnatal survival was followed for 21 days in *eNOS*$^{-/-}$, *eNOS*$^{+/-}$, and *eNOS*$^{+/+}$ mice (n=74, 81, and 60, respectively). Survival was significantly decreased in *eNOS*$^{-/-}$ and *eNOS*$^{+/-}$ compared with *eNOS*$^{+/+}$ mice with the same genetic background ($P<0.001$). Within 10 days after birth, 85.1% (63 of 74) of *eNOS*$^{-/-}$ and 38.3% (31 of 81) of *eNOS*$^{+/-}$ mice died, whereas only 13.3% (8 of 60) of *eNOS*$^{+/+}$ mice died during the same period ($P<0.001$, Figure 1A). These results demonstrated a dose-dependent effect between eNOS gene deficiency and postnatal mortality.

To determine if higher mortality observed in *eNOS*$^{-/-}$ was attributable to cardiac dysfunction, in vivo heart shortening was measured using the ultrasound crystals in *eNOS*$^{+/+}$, *eNOS*$^{+/-}$, and *eNOS*$^{-/-}$ mice at P1 (n=5 per group). Basal heart rate was similar among 3 groups (257±10, 284±18, and 252±15 beats/min, P=NS). Percent shortening of the heart was significantly decreased, whereas heart to chest ratio was increased in *eNOS*$^{-/-}$ compared with *eNOS*$^{+/+}$ mice (Figures 1B and 1C, $P<0.05$). Diastolic dimensions of the heart were significantly increased in *eNOS*$^{-/-}$ compared with *eNOS*$^{+/-}$ and *eNOS*$^{+/+}$ mice (3.37±0.04 versus 3.04±0.10 and 2.69±0.22 mm, respectively, $P<0.05$). Furthermore, LV and RV chamber size measured from serial sections of paraffin-embedded hearts at P1 was significantly increased in *eNOS*$^{-/-}$ compared with *eNOS*$^{+/+}$ mice (Figures 1D and 1E, n=5 per group, $P<0.05$). Dose-dependent relationship was evident between eNOS gene deficiency, heart shortening, and heart chamber size (Figures 1B through 1E). Postmortem examination showed that whereas lungs of *eNOS*$^{+/+}$ mice had normal and clear alveoli (Figure 1F), *eNOS*$^{-/-}$ mice had severe pulmonary congestion with focal alveolar edema (Figure 1G).

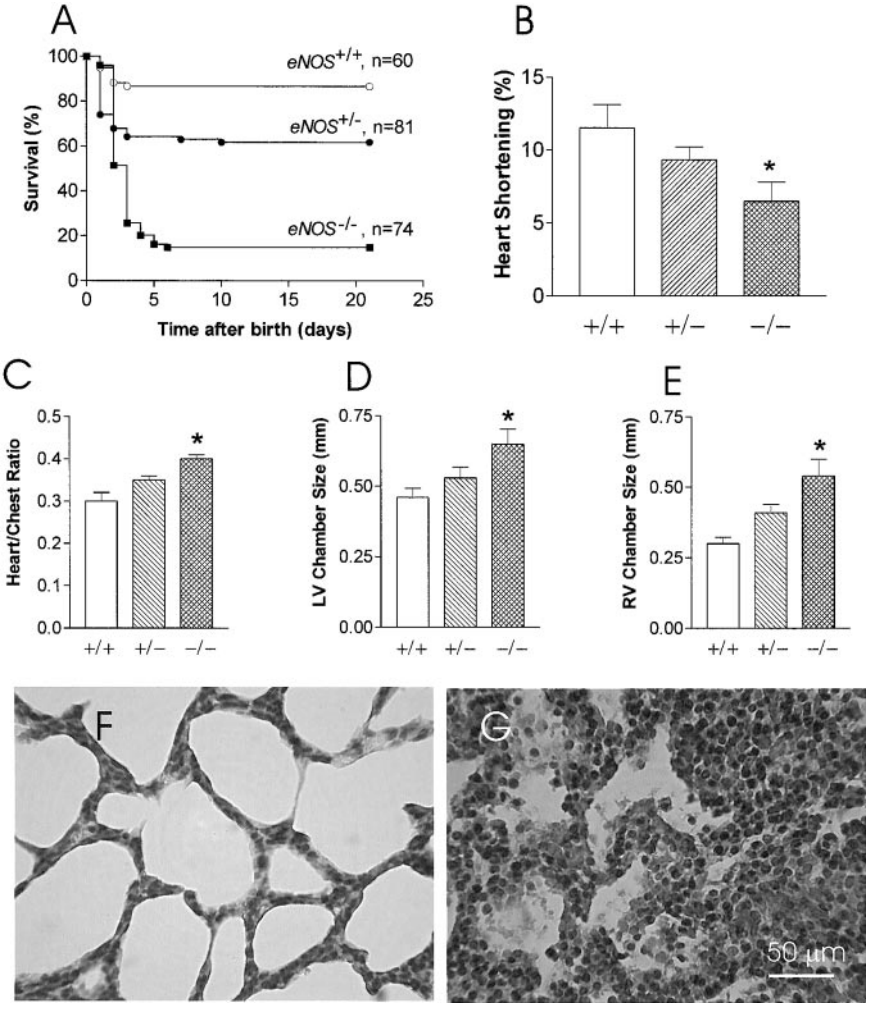

Figure 1. Postnatal survival, cardiac dysfunction, and pulmonary edema in $eNOS^{-/-}$ mice. A, Postnatal survival in $eNOS^{+/+}$, $eNOS^{+/-}$, and $eNOS^{-/-}$ mice. Animals were monitored for 21 days after birth. $P<0.001$ versus $eNOS^{+/+}$ mice. Heart shortening (B), heart/chest ratio (C), left ventricular (LV), and right ventricular (RV) chamber size (D and E) in neonatal $eNOS^{+/+}$, $eNOS^{+/-}$, and $eNOS^{-/-}$ mice (n=5 per group; *$P<0.05$ vs $eNOS^{+/+}$). F, Normal alveolar structures of neonatal $eNOS^{+/+}$ mice. G, Pulmonary congestion and edema in neonatal $eNOS^{-/-}$ mice. The alveolar capillaries of the lung were distended and filled with red blood cells. In some areas, the alveolar spaces were filled with fluids. F and G were stained with hematoxylin and eosin.

Congenital Septal Defects

Hearts were enlarged in $eNOS^{-/-}$ compared with $eNOS^{+/-}$ and $eNOS^{+/+}$ mice (Figure 2A). Serial heart sections were made in $eNOS^{-/-}$ and $eNOS^{+/+}$ mice at P2 (n=10 per group). A normal structure of the heart from an $eNOS^{+/+}$ mouse is shown in Figure 2B. Atrial or ventricular septal defects were found in 6 of 10 $eNOS^{-/-}$ mice, and only 1 of 10 $eNOS^{+/+}$ mice showed an atrial septal defect. Atrial septal defects were typical of ostium secundum defects (Figure 2C), ventricular septal defects were membranous and muscular defects in $eNOS^{-/-}$ mice (Figures 2D and 2E). Ventricular hypertrophy and enlargement of atria were obvious in $eNOS^{-/-}$ compared with $eNOS^{+/+}$ mice with congenital septal defects (Figures 2C through 2E).

Microdissections were performed in all mice at P1. In mice with atrial or ventricular septal defects, clear openings were observed in the atrial or ventricular septum that were not covered by any tissues. Congenital septal defects were additionally confirmed by scanning electron microscopy (Figure 3). The incidence of atrial or ventricular septal defects was significantly increased in $eNOS^{-/-}$ (75%) and $eNOS^{+/-}$ (32.4%) neonates compared with those of the $eNOS^{+/+}$ (4.9%, $P<0.001$). Whereas 11.2% of $eNOS^{-/-}$ neonates had ventricular septal defects, none were observed in the $eNOS^{+/-}$ and $eNOS^{+/+}$ mice (Table). These data demonstrated a dose-dependent relationship between eNOS gene deficiency and septal defects. No obvious defects were observed in tricuspid and mitral valves in $eNOS^{-/-}$ mice.

Caspase Activity and Apoptosis in the Developing Heart

To investigate possible mechanisms responsible for development of heart failure and congenital septal defects in $eNOS^{-/-}$ mice, we studied caspase-3 activity and myocardial apoptosis during embryonic development. To measure myocardial caspase-3 activity, embryonic hearts were collected from 4 pregnant $eNOS^{-/-}$ (22 hearts) and 3 pregnant $eNOS^{+/+}$ mice (21 hearts) at E12.5. Fetal hearts were also collected from 3 pregnant $eNOS^{-/-}$ (18 hearts) and 3 pregnant $eNOS^{+/+}$ mice (21 hearts) at E15.5. Caspase-3 activity was significantly higher in E12.5 and E15.5 myocardium from $eNOS^{-/-}$ compared with $eNOS^{+/+}$ mice (Figure 4, $P<0.05$). To determine apoptosis in the embryonic heart, TUNEL staining was performed in E12.5 hearts isolated from $eNOS^{-/-}$, $eNOS^{+/-}$, and $eNOS^{+/+}$ mice (n=5 to 7 per group). Representative TUNEL staining of fetal hearts from 3 groups is shown in Figure 5. Apoptosis was detected in the heart, including atrioventricular endothelial cushions, septum primum, and right and left ventricular myocardium in all 3 groups (Figure 5). However, apoptosis in these regions was significantly

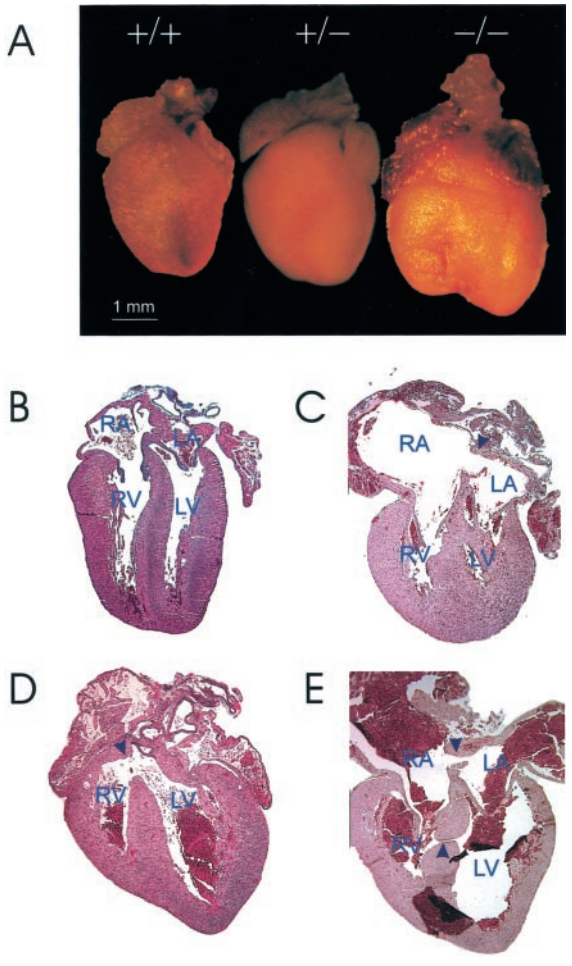

Figure 2. Atrial and ventricular septal defects in *eNOS*$^{-/-}$ mice. A, Gross external morphology of neonatal hearts isolated from *eNOS*$^{+/+}$ (left), *eNOS*$^{+/-}$ (middle), and *eNOS*$^{-/-}$ (right) mice at P2. Both right and left ventricles are markedly enlarged in the *eNOS*$^{-/-}$ compared with the *eNOS*$^{+/+}$ mouse. B through D, Frontal sections of neonatal hearts from P2 mice (original magnification ×50). B, Normal *eNOS*$^{+/+}$ mouse heart. C through E, Hearts from *eNOS*$^{-/-}$ mice. C, Atrial septal defect. D, Ventricular septal defect. E, Atrial and ventricular septal defects. Sections were stained with hematoxylin and eosin. Defects are indicated by arrows. RA indicates right atrium; RV, right ventricle; LA, left atrium; and LV, left ventricle.

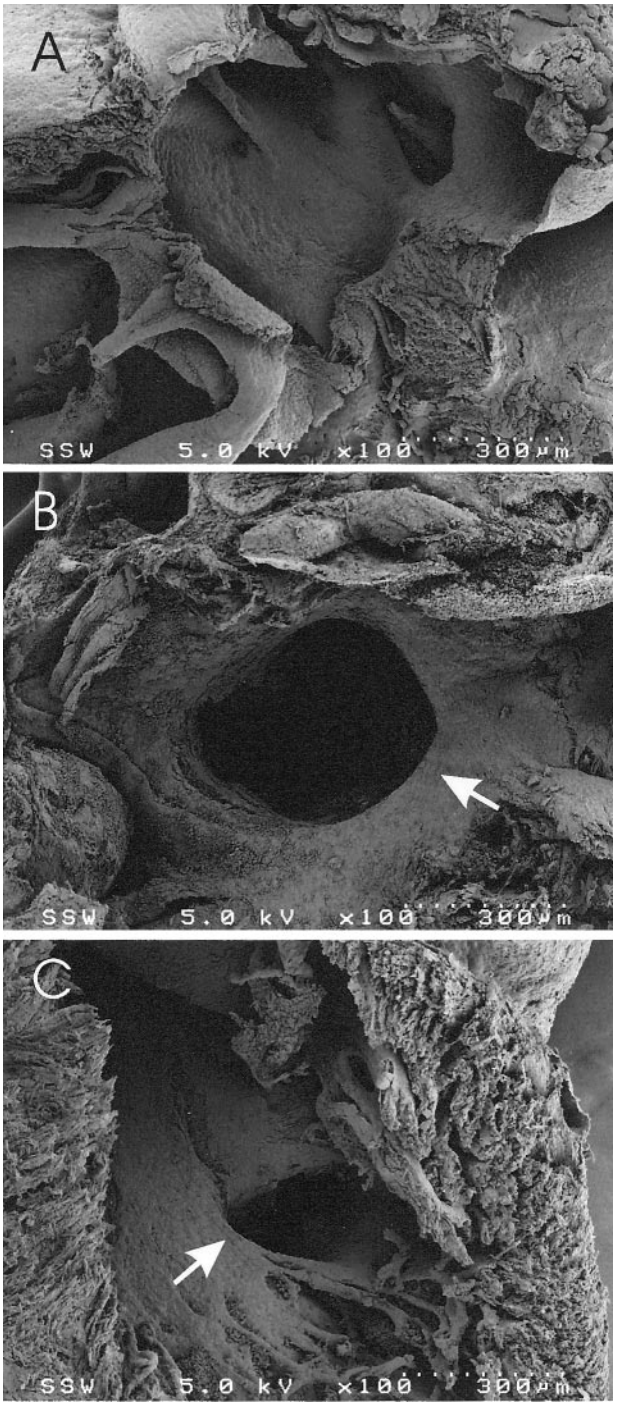

Figure 3. Identification of atrial and ventricular septal defects in *eNOS*$^{-/-}$ and *eNOS*$^{+/+}$ mice at P1 by scanning electron microscopy. A, Normal structure of atrial septum in an *eNOS*$^{+/+}$ mouse. B, Atrial septal defect in an *eNOS*$^{-/-}$ mouse. C, Ventricular septal defect (muscular type) in an *eNOS*$^{-/-}$ mouse. A and B are viewed from the right atrium. C is viewed from the left ventricle. Defects are indicated by arrows.

increased in *eNOS*$^{-/-}$ compared with *eNOS*$^{+/+}$ fetal hearts (Figure 6A, $P<0.01$). To additionally quantify the level of apoptosis during heart development, cell death detection ELISA assay was used. At E12.5, E15.5, and P1, apoptosis was significantly increased in the myocardium of *eNOS*$^{-/-}$ compared with *eNOS*$^{+/+}$ mice (Figure 6B, $P<0.05$).

Discussion

Ventricular and atrial septal defects are the most common forms of congenital heart disease (30% to 40%), affecting 1 to 2 in 200 live births in the United States.[23,24] Although the embryology of heart development has been described in some detail, the molecular mechanisms governing cardiac growth and morphogenesis remain largely unknown. The present study demonstrated for the first time that deficiency of eNOS led to significant increases in cardiomyocyte apoptosis and cardiac dysfunction. Furthermore, deficiency of eNOS gene increased congenital septal defects and postnatal mortality in a gene dosage–dependent manner. These results suggest that NO production from eNOS plays an important role in normal heart development.

Congenital Septal Defects in *eNOS*$^{+/+}$, *eNOS*$^{+/-}$ and *eNOS*$^{-/-}$ Neonatal Mice at P1

Genotype	*eNOS*$^{+/+}$	*eNOS*$^{+/-}$	*eNOS*$^{-/-}$
Normal	38 (95.1)	23 (67.6)*	9 (25.0)*
ASD	2 (4.9)	11 (32.4)*	23 (63.8)*
VSD	0 (0)	0 (0)	2 (5.6)
ASD and VSD	0 (0)	0 (0)	2 (5.6)
Total	41 (100)	34 (100)	36 (100)

Values are n (%).
ASD indicates atrial septal defects; VSD, ventricular septal defects.
*$P<0.001$ vs *eNOS*$^{+/+}$ by χ^2 analysis.

We started the present study by breeding the *eNOS*$^{-/-}$ and corresponding *eNOS*$^{+/+}$ controls, and we consistently obtained fewer *eNOS*$^{-/-}$ mice compared with *eNOS*$^{+/+}$ animals that survived to adulthood. Therefore, we began to monitor their breeding closely. To our surprise, most of the *eNOS*$^{-/-}$ newborns died within 6 days after birth. Mortality was markedly increased in *eNOS*$^{-/-}$ compared with the *eNOS*$^{+/+}$ neonates (85.5% versus 13.3%). To investigate if there is a dose-dependent effect between eNOS gene deficiency and postnatal mortality, *eNOS*$^{-/-}$ mice were bred with C57BL/6 mice to generate *eNOS*$^{+/-}$ animals. Consistent with our hypothesis, postnatal mortality of *eNOS*$^{+/-}$ mice was 38.3%, which was lower than *eNOS*$^{-/-}$ but higher than *eNOS*$^{+/+}$ mice. We additionally investigated the cause of death in the *eNOS*$^{-/-}$ neonates. Dose-dependent relationship was observed between eNOS gene deficiency and cardiac dysfunction, as measured by in vivo heart shortening. There was also a dose-dependent effect between eNOS deficiency and cardiac dilatation. Postmortem examination in mice that died after birth showed severe pulmonary congestion and edema in *eNOS*$^{-/-}$ mice. Our data indicate that death of *eNOS*$^{-/-}$ mice is most likely attributable to heart failure.

Congenital septal defects were observed in mice deficient in the eNOS gene. The septal defects include ostium secundum defects, ventricular septal defects (membranous and muscular type), and atrioventricular septal defects. Quantitative analysis demonstrated that congenital septal defects were found in 75% of *eNOS*$^{-/-}$, 32.4% of *eNOS*$^{+/-}$, and 4.9% of *eNOS*$^{+/+}$ mice. Our data showed a clear dose-dependent effect between eNOS gene deficiency and congenital septal defects, demonstrating an important role of eNOS in heart development. Although most *eNOS*$^{-/-}$ mice had atrial septal defects,

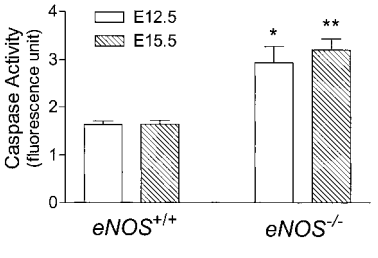

Figure 4. Caspase-3 activity in the developing heart of *eNOS*$^{-/-}$ and *eNOS*$^{+/+}$ mice at E12.5 and E15.5. To make each measurement, 5 to 7 hearts were pooled; 3 to 4 independent measurements were made in each group. *$P<0.05$, **$P<0.01$ vs *eNOS*$^{+/+}$ mice.

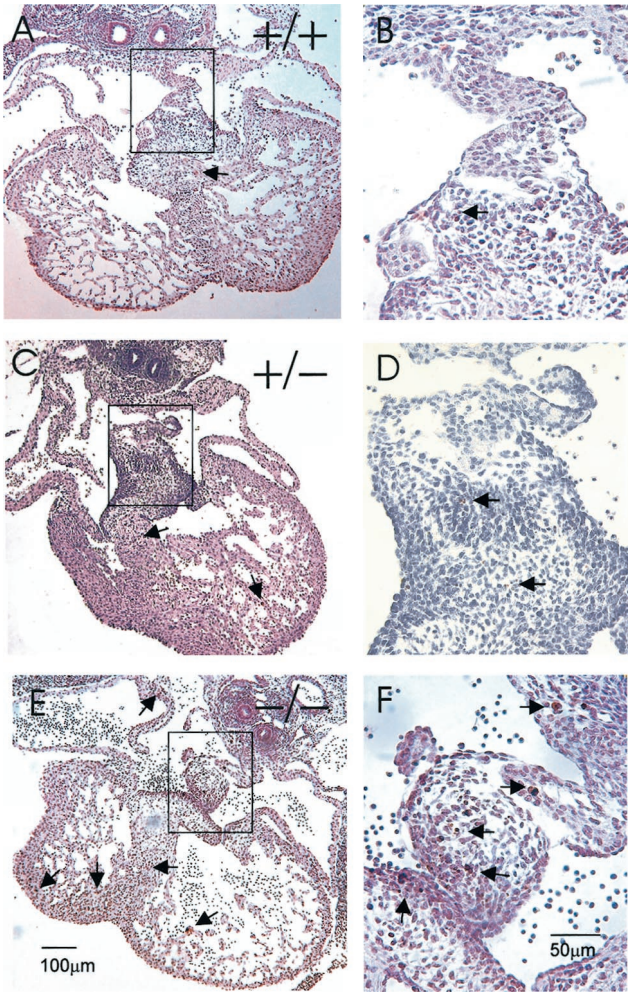

Figure 5. Apoptosis in the myocardium of fetal *eNOS*$^{+/+}$, *eNOS*$^{+/-}$, and *eNOS*$^{-/-}$ mice at E12.5. Top, middle, and bottom panels represent *eNOS*$^{+/+}$ (A and B), *eNOS*$^{+/-}$ (C and D), and *eNOS*$^{-/-}$ mice (E and F), respectively. Apoptosis determined by TUNEL staining was detected in the heart, including atrioventricular endothelial cushions, septum primum, and right and left ventricular myocardium in all 3 groups. Arrows indicate apoptotic nuclei. However, *eNOS*$^{-/-}$ had more apoptosis compared with *eNOS*$^{+/+}$ and *eNOS*$^{+/-}$ mice. The area of septum primum and atrioventricular endothelial cushions (the boxed area) in A, C, and E is enlarged to B, D and F, respectively.

it is unlikely that atrial septal defects alone resulted in cardiac dysfunction and high mortality in these animals. The lack of a complete penetrance also suggested that, in addition to eNOS, other modifier genes are involved in heart failure and congenital septal defects during development.

Mechanisms by which heart failure and congenital septal defects develop in *eNOS*$^{-/-}$ mice are not known. Apoptosis is an important physiological process in organ development. During early embryonic and postnatal heart development, apoptosis is demonstrated in several areas, including atrioventricular endothelial cushions, the outflow tract, septum, and trabeculae, as well as papillary muscles of ventricules.[11–15] This is a highly regulated process, because increased apoptosis may result in congenital heart defects. Studies demonstrated that intra-amniotic treatment of cyclophosphamide increased apoptosis in atrioventricular endothe-

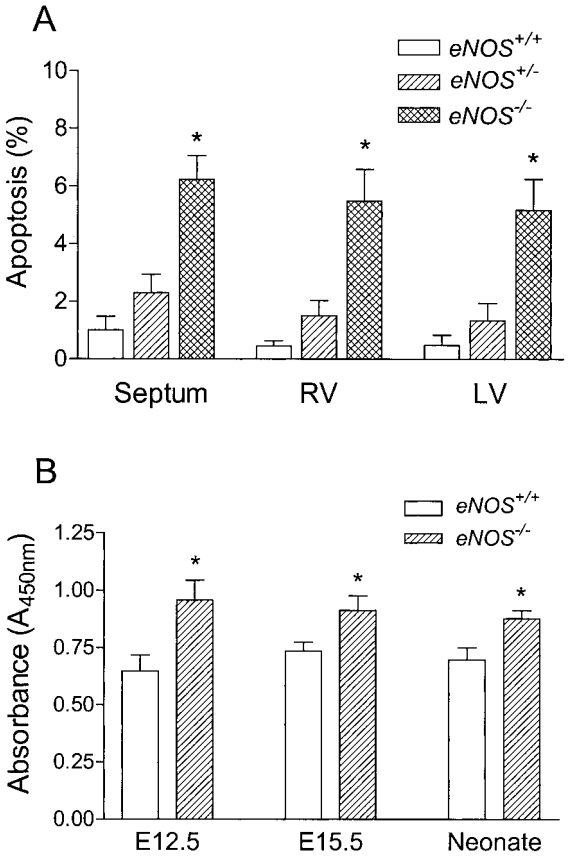

Figure 6. Myocardial apoptosis in *eNOS*$^{-/-}$, *eNOS*$^{+/-}$, and *eNOS*$^{+/+}$ mice. A, Apoptosis determined by TUNEL staining at E12.5. Apoptosis was significantly increased in atrioventricular endothelial cushion and septum primum (septum) and right and left ventricular myocardium (RV and LV) in *eNOS*$^{-/-}$ compared with *eNOS*$^{+/-}$ and *eNOS*$^{+/+}$ mice (n=5 to 7, **P*<0.01). B, Quantitative analysis of apoptosis by cell death detection ELISA in the heart at E12.5, E15.5, and P1 (neonate). Apoptosis was significantly increased at all time points in *eNOS*$^{-/-}$ compared with *eNOS*$^{+/+}$ mice (n=6 to 9 per group, **P*<0.05).

lial cushions and proximal left bulbar cushions of the developing heart in chick embryos, and this resulted in 75% of ventricular septal defects.[11] To investigate if cardiomyocyte apoptosis plays a role in the development of heart failure and septal defects in *eNOS*$^{-/-}$ mice, we measured apoptosis during heart development. Apoptosis was significantly increased in the heart at E12.5, E15.5, and P1. TUNEL staining indicated that apoptosis was increased in the whole heart, including atrioventricular endothelial cushions, septum primum, and ventricular myocardium in *eNOS*$^{-/-}$ mice. One of the hallmarks of apoptosis is caspase activation. Activation of caspase-3, -6, and -7 is considered as a point of no return in the process leading to DNA cleavage and cell destruction.[25,26] In the present study, we demonstrated that caspase-3 activity was significantly increased in E12.5 and E15.5 hearts in *eNOS*$^{-/-}$ compared with *eNOS*$^{+/+}$ mice. Our results suggested that increased cardiomyocyte apoptosis during embryonic development is involved in development of heart failure and congenital septal defects in *eNOS*$^{-/-}$ mice. It is not clear why defects only occurred in the septum. This may be attributable to the fact that the septum area has thin muscle layers compared with the rest of the ventricles and thus is more susceptible to structural damages by increasing apoptosis.

Mice deficient in eNOS also exhibit limb reduction defects.[27] These limb abnormalities were observed in ≈10% of *eNOS*$^{-/-}$ mice. Furthermore, Lee et al[17] recently showed that 42% of *eNOS*$^{-/-}$ mice exhibit a bicuspid aortic valve. The presence of atrial or ventricular septal defects and a bicuspid aortic valve together with abnormal limb development in the *eNOS*$^{-/-}$ mice resembles the abnormalities in patients with Holt-Oram syndrome (the heart-hand syndrome).[28,29] Decreased basal NO production may contribute to abnormalities found in Holt-Oram syndrome in some patients.

In summary, the present study demonstrated that deficiency in eNOS results in heart failure and congenital septal defects. Our data suggest that NO production from eNOS plays an important role in normal heart development. Increased apoptosis during embryonic development represents one of the mechanisms that leads to heart failure and congenital septal defects in *eNOS*$^{-/-}$ mice.

Acknowledgments

This study was supported by grants awarded to Dr Qingping Feng from the Canadian Institutes of Health Research (grant MT-14653) and the Heart and Stroke Foundation of Ontario (grant T4045). We thank Paul Coakwell and Dean Worsfold for expert animal care.

References

1. Feng Q, Hedner T. Endothelium-derived relaxing factor (EDRF) and nitric oxide (NO), I: physiology, pharmacology and pathophysiological implications. *Clin Physiol*. 1990;10:407–426.
2. Forstermann U, Close EI, Pollock JS, et al. Nitric oxide synthase isozymes: characterization, purification, molecular cloning, and functions. *Hypertension*. 1994;23:1121–1131.
3. Bloch W, Fleischmann BK, Lorke DE, et al. Nitric oxide synthase expression and role during cardiomyogenesis. *Cardiovasc Res*. 1999;43: 675–684.
4. Balligand JL, Kelly RA, Marsden PA, et al. Control of cardiac muscle cell function by an endogenous nitric oxide signaling system. *Proc Natl Acad Sci U S A*. 1993;90:347–351.
5. Kanai AJ, Mesaros S, Finkel MS, et al. β-adrenergic regulation of constitutive nitric oxide synthase in cardiac myocytes. *Am J Physiol*. 1997;273:C1371–C1377.
6. Kelly RA, Balligand JL, Smith TW. Nitric oxide and cardiac function. *Circ Res*. 1996;79:363–380.
7. Paulus WJ, Shah AM. NO and cardiac diastolic function. *Cardiovasc Res*. 1999;43:595–606.
8. Murohara T, Asahara T, Silver M, et al. Nitric oxide synthase modulates angiogenesis in response to tissue ischemia. *J Clin Invest*. 1998;101: 2567–2578.
9. Dimmeler S, Haendeler J, Nehls M, et al. Suppression of apoptosis by nitric oxide via inhibition of interleukin-1β-converting enzyme (ICE)-like and cysteine protease protein (CPP)-32-like proteases. *J Exp Med*. 1997; 185:601–607.
10. Kim Y-M, Talanian RV, Billiar TR. Nitric oxide inhibits apoptosis by preventing increases in caspase-3-like activity via two distinct mechanisms. *J Biol Chem*. 1997;272:31138–31148.
11. Pexieder T. Cell death in the morphogenesis and teratogenesis of the heart. *Adv Anat Cell Biol*. 1975;51:1–99.
12. Watanabe M, Choudhry A, Berlan M, et al. Developmental remodeling and shortening of the cardiac outflow tract involves myocyte programmed cell death. *Development*. 1998;125:3809–3820.
13. Abdelwahid E, Pelliniemi LJ, Niinikoski H, et al. Apoptosis in the pattern formation of the ventricular wall during mouse heart organogenesis. *Anat Rec*. 1999;256:208–217.
14. Zhao Z, Rivkees SA. Programmed cell death in the developing heart: regulation by BMP4 and FGF2. *Dev Dyn*. 2000;217:388–400.
15. Kajstura J, Mansukhani M, Cheng W, et al. Programmed cell death and expression of the protooncogene bcl-2 in myocytes during postnatal maturation of the heart. *Exp Cell Res*. 1995;219:110–121.

16. Webb S, Brown NA, Anderson RH. Formation of the atrioventricular septal structures in the normal mouse. *Circ Res*. 1998;82:645–656.
17. Lee TC, Zhao YD, Courtman DW, et al. Abnormal aortic valve development in mice lacking endothelial nitric oxide synthase. *Circulation*. 2000;101:2345–2348.
18. Pexieder T. Standardized method for study of normal and abnormal cardiac development in chick, rat, mouse, dog and human embryos. *Teratology*. 1986;33:91C–92C.
19. Gruber PJ, Kubalak SW, Pexieder T, et al. RXR α deficiency confers genetic susceptibility for aortic sac, conotruncal, atrioventricular cushion, and ventricular muscle defects in mice. *J Clin Invest*. 1996;98:1332–1343.
20. Feng Q, Lu X, Jones DL, et al. Increased inducible nitric oxide synthase expression contributes to myocardial dysfunction and higher mortality post-myocardial infarction in mice. *Circulation*. 2001;104:700–704.
21. Song W, Lu X, Feng Q. Tumor necrosis factor-α induces apoptosis via inducible nitric oxide synthase in neonatal mouse cardiomyocytes. *Cardiovasc Res*. 2000;45:595–602.
22. Bradford MM. A rapid and sensitive method for the quantitation of microgram quantities of protein utilizing the principle of protein-dye binding. *Anal Biochem*. 1976;72:248–254.
23. Payne RM, Johnson MC, Grant JW, et al. Toward a molecular understanding of congenital heart disease. *Circulation*. 1995;91:494–504.
24. Edwards WD. Congenital heart disease. In: Damjanov I, Linder J, eds. *Anderson's Pathology*. 10th ed. St Louis, Mo: Mosby-Year Book Inc; 1996:1339–1396.
25. Enari M, Sakahira H, Yokoyama H, et al. A caspase-activated DNase that degrades DNA during apoptosis, and its inhibitor ICAD. *Nature*. 1998; 391:43–50.
26. Schwartz SM. Cell death and the caspase cascade. *Circulation*. 1998;97: 227–229.
27. Gregg AR, Schauer A, Shi O, et al. Limb reduction defects in endothelial nitric oxide synthase-deficient mice. *Am J Physiol*. 1998;275: H2319–H2324.
28. Basson CT, Cowley GS, Solomon SD, et al. The clinical and genetic spectrum of the Holt-Oram syndrome (heart-hand syndrome). *N Engl J Med*. 1994;330:885–891.
29. Gelb BD, Zhang J, Sommer RJ, et al. Familial patent ductus arteriosus and bicuspid aortic valve with hand anomalies: a novel heart-hand syndrome. *Am J Med Genet*. 1999;87:175–179.